

The pion electromagnetic form factor

Frederic D. R. Bonnet^{a,b}, Robert G. Edwards^b, George T. Fleming^b, Randy Lewis^a, David G. Richards^b

^aDepartment of Physics, University of Regina, Regina, SK, S4S 0A2, Canada

^bThomas Jefferson National Accelerator Facility, Newport News, VA 23606, USA

A ratio of lattice correlation functions is identified from which the pion form factor can be obtained directly. Preliminary results from quenched Wilson simulations are presented.

1. MOTIVATION

The pion form factor is a convenient way to study the transition from perturbative to non-perturbative QCD. This transition is typically expected to occur at a smaller Q^2 than for the nucleon, and should thus be more easily attainable in experiments and in lattice studies. Also, the asymptotic normalization of the pion form factor is known in terms of f_π . In addition, lattice simulations of the pion form factor benefit from the complete absence of “disconnected” quark diagrams.[1]

Some experimental data already exist, another experiment is in progress right now at Jefferson Lab, and measurements at higher Q^2 are planned for the future.[2].

Pioneering lattice QCD studies were carried out in the 1980’s[1,3,4], and only recently has the pion form factor been revisited using lattice methods.[5,6] In light of the substantial experimental effort, it is important to produce lattice QCD results with significantly smaller quark masses than have yet been employed, and eventually to attain larger values of Q^2 . Unquenched simulations will also be important. Here, after a general discussion of correlation functions, the issue of smaller quark masses will be addressed using quenched Wilson data.

2. CORRELATION FUNCTIONS

The electromagnetic form factor is obtained in lattice QCD simulations by placing a charged pion creation operator at Euclidean time t_i , a charged pion annihilation operator at t_f , and a

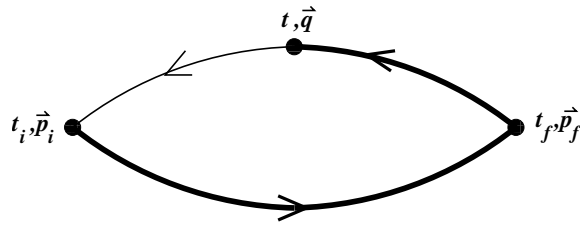


Figure 1. The quark propagators used to compute the pion form factor.

vector current insertion at t as shown in Fig. 1. A standard determination of 12 columns in the inverse of the quark matrix provides the two propagators that originate from t_i . The remaining propagator is obtained for any particular annihilation operator, having definite momentum \vec{p}_f , by a two step procedure: the propagator from t_i to t_f is multiplied by the annihilation operator and that product is used as the input for a second 12-column linear algebra step. This determines the entire thick quark line of Fig. 1. The momenta at the source (\vec{p}_i) and at the insertion (\vec{q}) can then be varied freely without computing new propagators. Since the largest Q^2 is attained in the Breit frame ($\vec{p}_f = -\vec{p}_i$), the simple choice of $\vec{p}_f = \vec{0}$ is not always desirable.

The form factor, $F(Q^2)$, is defined by

$$\begin{aligned} \langle \pi(\vec{p}_f) | V_\mu(0) | \pi(\vec{p}_i) \rangle_{\text{continuum}} & \quad (1) \\ & = Z_V \langle \pi(\vec{p}_f) | V_\mu(0) | \pi(\vec{p}_i) \rangle = F(Q^2)(p_i + p_f)_\mu \end{aligned}$$

where $V_\mu(x)$ is the chosen vector current. $F(Q^2)$ can be extracted from ratios of lattice correlation

functions. The three-point correlator is

$$\Gamma_{\pi\mu\pi}^{AB}(t_i, t, t_f, \vec{p}_i, \vec{p}_f) = a^9 \sum_{\vec{x}_i, \vec{x}_f} e^{-i(\vec{x}_f - \vec{x}) \cdot \vec{p}_f} \times e^{-i(\vec{x} - \vec{x}_i) \cdot \vec{p}_i} \langle 0 | \phi_B(x_f) V_\mu(x) \phi_A^\dagger(x_i) | 0 \rangle \quad (2)$$

where $A \in (L, S)$ and $B \in (L, S)$ denote either “local” or “smeared”. Inserting complete sets of hadron states and requiring $t_i \ll t \ll t_f$, gives

$$\Gamma_{\pi\mu\pi}^{AB}(t_i, t, t_f, \vec{p}_i, \vec{p}_f) \rightarrow \langle 0 | \phi_B(x) | \pi(\vec{p}_f) \rangle \times \langle \pi(\vec{p}_f) | V_\mu(x) | \pi(\vec{p}_i) \rangle \langle \pi(\vec{p}_i) | \phi_A^\dagger(x) | 0 \rangle \times \frac{a^3}{4E_f E_i} e^{-(t_f - t)E_f} e^{-(t - t_i)E_i}. \quad (3)$$

Similarly for the two-point correlator,

$$\Gamma_{\pi\pi}^{AB}(t_i, t_f, \vec{p}) \rightarrow \langle 0 | \phi_B(x_i) | \pi(\vec{p}) \rangle \times \langle \pi(\vec{p}) | \phi_A^\dagger(x_i) | 0 \rangle \frac{a^3}{2E} e^{-(t_f - t_i)E}. \quad (4)$$

Finally, consider operators that are temporally local, but spatially smeared democratically among the three spatial axes:

$$a^2 \langle 0 | \phi_L(x) | \pi(\vec{p}) \rangle = Z_L e^{ix \cdot p}, \quad (5)$$

$$a^2 \langle 0 | \phi_S(x) | \pi(\vec{p}) \rangle = Z_S (|\vec{p}|) e^{ix \cdot p}. \quad (6)$$

From this discussion, it is found that the following expression for the form factor is independent of Z_L , $Z_S(|\vec{p}|)$, and all time exponentials:

$$F(Q^2) = \frac{\Gamma_{\pi 4\pi}^{AB}(t_i, t, t_f, \vec{p}_i, \vec{p}_f) \Gamma_{\pi\pi}^{CL}(t_i, t, \vec{p}_f)}{\Gamma_{\pi\pi}^{AL}(t_i, t, \vec{p}_i) \Gamma_{\pi\pi}^{CB}(t_i, t_f, \vec{p}_f)} \times \left(\frac{2Z_V E_f}{E_i + E_f} \right), \quad (7)$$

where the indices A , B and C can be either L (local) or S (smeared). For a conserved current, $Z_V \equiv 1$.

3. ACTION AND PARAMETERS

Our initial explorations have used the (quenched) Wilson action with $\beta = 6$, so $a \sim 0.10$ fm. Periodic boundary conditions are used except for the quark temporal boundaries, which are Dirichlet. Hopping parameters and lattice sizes are shown in Table 1; the resulting pseudoscalar and vector meson masses are also listed.

Table 1

The chosen hopping parameters and numbers of lattice sites, along with the computed pseudoscalar and vector meson masses.

κ	lattice	am_{PS}	am_V
0.1480	$16^3 \times 32$	0.673	0.712
0.1520	$16^3 \times 32$	0.477	0.549
0.1540	$16^3 \times 32$	0.364	0.468
0.1555	$24^3 \times 32$	0.259	0.398
0.1563	$24^3 \times 32$	0.179	0.358
0.1566	$24^3 \times 32$ & $32^3 \times 48$	0.145	0.343

Notice that the smallest pion mass is less than 300 MeV, and therefore significantly below those used in previous studies of the pion form factor. The pion operators are fixed at $t_i = 7$ and $t_f = 21$ except for the $32^3 \times 48$ lattices, where $t_f = 28$. The standard point-split conserved vector current is used. A gauge-covariant Gaussian smearing is employed at the source,

$$b(x) \rightarrow \left(1 + \frac{\omega \vec{\nabla} U}{N} \right)^N b(x). \quad (8)$$

The various results shown here are based on the analysis of between 80 and 155 configurations.

4. PRELIMINARY RESULTS

Representative plots of the data are shown in Fig. 2. For each of the smaller hopping parameters, there is a reasonable plateau at timesteps sufficiently far from the pion operators (timesteps 0 and 14). For $\kappa = 0.1563$ and 0.1566 , the possible plateau spans only a few timesteps.

Correlated fits to the data have produced Fig. 3 which shows the form factor as a function of Q^2 for each available κ . For comparison, the monopole curve $1/(1 + Q^2/m_\rho^2)$ is also shown where m_ρ denotes the physical ρ meson mass. Notice that the experimental measurements from Ref. [7] lie on the monopole curve. For each κ the lattice results also display a monopole form, and $F(Q^2)$ is found to decrease with decreasing quark mass as expected since the effective vector meson mass of the monopole form also shrinks with decreasing quark mass.

In conclusion, Eq. (7) is found to be a useful

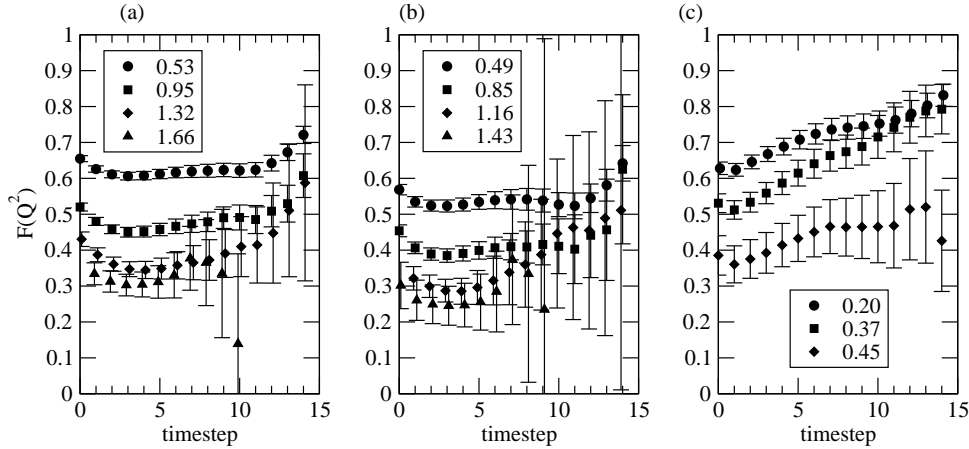


Figure 2. Pion form factor data versus timestep, for (a) $\kappa=0.1520$, (b) $\kappa=0.1540$ and (c) $\kappa=0.1563$. Numerical values of Q^2 in GeV^2 are shown in the legends.

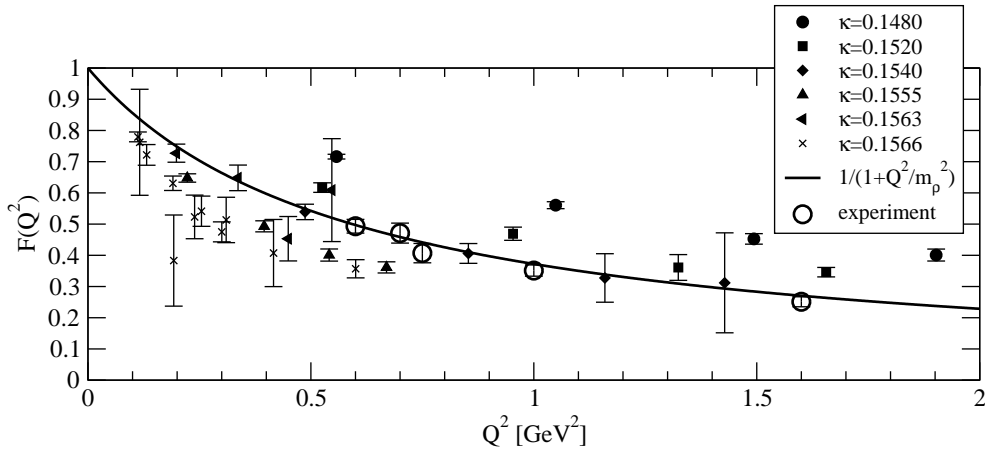


Figure 3. Results for the pion form factor as a function of Q^2 for each of the available κ values. Experimental measurements[7] and the monopole approximation are also shown.

method for extracting the pion form factor. Simulations with domain-wall fermions are underway.

This work was supported in part by the Natural Sciences and Engineering Research Council of Canada and by the U.S. Department of Energy under contract DE-AC05-84ER40150. Computations were performed on the 128-node Pentium IV cluster at JLab.

REFERENCES

1. T. Draper, R. M. Woloshyn, W. Wilcox and K.-F. Liu, Nucl. Phys. B318, 319 (1989).
2. For a review, see H. P. Blok, G. M. Huber and D. J. Mack, nucl-ex/0208011.
3. W. Wilcox and R. M. Woloshyn, Phys. Rev. Lett. 45, 2653 (1985); R. M. Woloshyn and A. M. Kobos, Phys. Rev. D33, 222 (1986); R. M. Woloshyn, Phys. Rev. D34, 605 (1986).
4. G. Martinelli and C. T. Sachrajda, Nucl. Phys. B306, 865 (1988).
5. J. van der Heide, M. Lutterot, J. H. Koch and E. Laermann, hep-lat/0303006.
6. Y. Nemoto (RBC Collaboration), these proceedings.
7. J. Volmer et al., Phys. Rev. Lett. 86, 1713 (2001).